Research Article

Ghada ALMisned, Gulfem Susoy, Hesham M. H. Zakaly, Elaf Rabaa, Gokhan Kilic, Erkan Ilik, Duygu Sen Baykal, Antoaneta Ene*, Huseyin Ozan Tekin*

The role of Ag_2O incorporation in nuclear radiation shielding behaviors of the Li_2O–Pb_3O_4–SiO_2 glass system: A multi-step characterization study

https://doi.org/10.1515/chem-2022-0354
received May 9, 2023; accepted June 18, 2023

Abstract: We report the gamma-ray shielding properties of five different lithium silicate glasses based on the $(40 - x)$ Li_2O–$10Pb_3O_4$–$50SiO_2$ nominal composition. Transmission factor values and some basic shielding parameters such as linear (μ) and mass attenuation coefficients (μ/ρ), half-value layer, tenth value layer, and mean free path (MFP) values of the investigated glass samples are determined in a large photon energy range. Using the G–P fitting method at various MFP values, the exposure buildup factor and energy absorption buildup factor values of the examined glasses are also calculated. Based on the findings, it can be concluded that the S5 glass specimen, which exhibits the greatest Ag_2O additive and density among the various glass samples, represents a favorable choice for the purpose of shielding against gamma radiation.

Keywords: lithium silicate glass, Ag_2O, Phy-X/PSD, MCNPX, radiation shielding, EABF, EBF

*** Corresponding author: Antoaneta Ene**, Department of Chemistry, Physics and Environment, INPOLDE Research Center, Faculty of Sciences and Environment, Dunarea de Jos University of Galati, 47 Domneasca Street, 800008 Galati, Romania, e-mail: Antoaneta.Ene@ugal.ro
*** Corresponding author: Huseyin Ozan Tekin**, Medical Diagnostic Imaging Department, College of Health Sciences, University of Sharjah, Sharjah, 27272, United Arab Emirates; Computer Engineering Department, Faculty of Engineering and Natural Sciences, Istinye University, Istanbul 34396, Turkey, e-mail: tekin765@gmail.com
Ghada ALMisned: Department of Physics, College of Science, Princess Nourah Bint Abdulrahman University, P.O. Box 84428, Riyadh 11671, Saudi Arabia
Gulfem Susoy: Department of Physics, Faculty of Science, Istanbul University, Istanbul, Turkey
Hesham M. H. Zakaly: Institute of Physics and Technology, Ural Federal University, 620002 Ekaterinburg, Russia; Physics Department, Faculty of Science, Al-Azhar University, Assiut 71524, Egypt
Elaf Rabaa: Medical Diagnostic Imaging Department, College of Health Sciences, University of Sharjah, Sharjah, 27272, United Arab Emirates
Gokhan Kilic, Erkan Ilik: Department of Physics, Faculty of Science, Eskisehir Osmangazi University, TR-26040 Eskisehir, Turkey
Duygu Sen Baykal: Mechatronics Engineering, Faculty of Engineering and Architecture, Istanbul Nisantasi University, 34398, Istanbul, Turkey

1 Introduction

Lithium silicate glass is a type of glass that contains lithium oxide (Li_2O) and silicon dioxide (SiO_2) as its primary components [1,2]. It is also known as lithium disilicate glass or simply lithium glass. Lithium silicate glass has several desirable properties that make it useful in a variety of applications such as dentistry and electronics [3–7]. For instance, it has a low coefficient of thermal expansion, meaning that it can withstand rapid temperature changes without cracking. It is also highly resistant to chemical corrosion and has excellent mechanical strength. In dentistry, lithium silicate glass is used to create restorative dental crowns, bridges, and veneers. It is a popular choice because it can be milled and polished to a high degree of precision, resulting in a natural-looking tooth restoration that is both durable and biocompatible [8–11]. In electronics, lithium silicate glass is used as a substrate for thin-film transistors and other microelectronic components [12–15]. Its thermal and chemical properties make it a good choice for applications where high temperatures and harsh chemicals are present. Meanwhile, the literature suggests that the production of glass materials for the purpose of radiation protection is becoming more widely recognized [16–21]. Through the manipulation of glass densities, while maintaining optimal optical properties, several studies have facilitated the development of numerous novel and auspicious glass materials. Radiation shielding glasses are to protect workers and devices from ionizing radiation. They are mostly made with heavy glasses that

contain a specific number of oxides, which absorb harmful radiation before it can reach the living biological tissue. Radiation shielding glasses are used in a variety of facilities, where exposure to ionizing radiation is a concern, such as medical imaging facilities, dental clinics, and veterinary clinics [22–30]. It is important to note that radiation shielding glasses are not a substitute for other forms of personal protective equipment, such as lead (Pb) aprons or other shields. They are designed to work in conjunction with these other forms of protection to ensure maximum safety for the wearer. The primary goal of radiation protection is to limit the dose of radiation that a person receives to a level that is considered safe. This is done through a combination of administrative controls (such as limiting the amount of time a person spends near a radiation source), engineering controls (such as shielding or containment), and personal protective equipment (such as radiation shielding garments or eyewear) [31–34]. The level of radiation exposure that is considered safe depends on a variety of factors, including the type of radiation, the duration of exposure, and the age and health of the person being exposed. Regulatory agencies such as the International Atomic Energy Agency and the Nuclear Regulatory Commission establish guidelines and regulations for safe levels of radiation exposure [35–37]. In addition to protecting individuals who are working with or around sources of radiation, radiation protection is also important in the event of a radiological emergency, such as a nuclear accident. Emergency responders and other personnel may use specialized equipment and procedures to minimize the spread of radiation and protect themselves and others from exposure. The objective of this investigation is to analyze the impact of lithium silicate glasses and structurally modified alterations on radiation absorption characteristics, as documented in previous research, with a focus on scrutinizing certain crucial properties. Considering the promising features of lithium silicate glasses for shielding applications such as high durability against chemical corrosion and excellent mechanical strength, the acquisition of data from the study has the potential to enhance comprehension of the gamma-ray absorption characteristics exhibited by these beneficial glasses.

2 Materials and methods

A thorough investigation was done on the gamma-ray shielding capabilities of five different glasses with the chemical formula $(40 - x)Li_2O$–$10Pb_3O_4$–$50SiO_2$ (where x = 0–0.4 mol%). Studies have been done on the effects of adding a modest concentration of Ag_2O to lithium silicate glasses on gamma shielding. The codes for the five different lithium silicate glass samples that were used are S1, S2, S3, S4, and S5. According to the referenced research [38], the densities of glass samples S1, S2, S3, S4, and S5 were 3,998, 4,027, 4,031, 4,038, and 4,083 g/cm^3 (Table 1). The technical information and estimated parameters for nuclear radiation shielding are shown here. Phy-X PSD software was used to determine the radiation attenuation parameters of the samples [39].

Table 1: Chemical properties of the investigated glasses [38]

Sample code	Weight fraction (mol%)				Density ρ (±0.001) (g/cm^3)
	$(40 - x)Li_2O$	$10Pb_3O_4$	$50SiO_2$	xAg_2O	
S1	40.0	10	50.0	0.0	3.998
S2	39.9	10	50.0	0.1	4.027
S3	39.8	10	50.0	0.2	4.031
S4	39.7	10	50.0	0.3	4.038
S5	39.6	10	50.0	0.4	4.083

2.1 Investigated gamma-ray shielding parameters

The linear attenuation coefficient (μ) is a measure of how strongly a material attenuates or weakens a beam of radiation as it passes through the material. It represents the fraction of the incident radiation that is absorbed or scattered per unit length of the material. The linear attenuation coefficient is dependent on both the type of radiation and the material it is passing through. Different types of radiations, such as gamma rays or X-rays, may have different linear attenuation coefficients in the same material due to their different energies and interaction mechanisms with the material. The linear attenuation coefficient is typically measured in units of inverse length, such as cm^{-1} or m^{-1}. It can be calculated using the following formula [40]:

$$\mu = \frac{\ln\left(\frac{I_0}{I}\right)}{d}, \tag{1}$$

where μ is the linear attenuation coefficient, I_0 is the intensity of the incident radiation, I is the intensity of the transmitted radiation, and d is the thickness of the material. The linear attenuation coefficient is an important parameter in radiation shielding calculations, as it is used to determine the amount of radiation that will be absorbed or scattered

by a particular material and the thickness required to achieve a desired level of radiation protection. Like the linear attenuation coefficient, the mass attenuation coefficient (μ_m) is dependent on both the type of radiation and the material it is passing through. Different types of radiations, such as gamma rays or X-rays, may have different mass attenuation coefficients in the same material due to their different energies and interaction mechanisms with the material. We calculated the (μ_m) values of the glass samples using the obtained μ values to determine their density-independent radiation attenuation properties [41]:

$$\mu_m = \frac{\mu}{\rho}. \tag{2}$$

The half-value layer (HVL) is a measure of the penetration power of a beam of radiation through a material. It is defined as the thickness of the material required to reduce the intensity of the radiation to half of its original value. The HVL depends on the energy of the radiation and the material it is passing through. Materials with high atomic numbers and densities, such as lead, typically have a smaller HVL [42] for a given type of radiation compared to materials with lower atomic numbers and densities, such as water or air. The build-up factor is a correction factor used in radiation shielding calculations to account for the additional scattering of radiation that occurs within a shielded material. As a beam of radiation passes through a material, it interacts with the atomic and molecular structures of the material, causing some of the radiation to be scattered in different directions. The build-up factor (energy absorption build-up factor [EABF] and exposure build-up factor [EBF]) considers this scattered radiation and provides a correction factor to the shielding thickness required to achieve a desired level of radiation protection. The build-up factor is dependent on both the energy and type of radiation and the material it is passing through [43–45]. It is typically measured experimentally using a radiation detector and a series of shielding materials. The gamma-ray transmission factor (TF), also known as the gamma-ray transmittance, is a measure of the fraction of incident gamma radiation that passes through a material without being absorbed or scattered. It is expressed as a percentage and can be used to calculate the intensity of gamma radiation that will be transmitted through a given thickness of material. The gamma-ray TF is dependent on both the energy of the gamma radiation and the material it is passing through. Higher-energy gamma radiation typically has a higher TF than lower-energy gamma radiation for a given material, while denser materials with higher atomic numbers typically have a lower TF than lighter materials for a given energy of gamma radiation. The gamma-ray TF can be calculated using the following formula:

$$T = \left(\frac{I}{I_0}\right) \times 100\%, \tag{3}$$

where T is the gamma-ray TF, I is the intensity of the transmitted gamma radiation, and I_0 is the intensity of the incident gamma radiation.

The gamma-ray TF is an important parameter in radiation shielding calculations, as it is used to determine the thickness and density of materials required to achieve a desired level of radiation protection. In general, a higher gamma-ray TF means that less shielding material is required to achieve the desired level of radiation protection. Previous studies in the literature can be used to find the technical and theoretical details concerning the crucial gamma-ray absorption parameters calculated in this work [46–50].

2.2 Monte Carlo simulation through MCNPX code

MCNPX (Monte Carlo N-Particle eXtended) [51] is a computer code used for simulating the transport of particles through matter, particularly in the fields of nuclear engineering and health physics. It is a widely used Monte Carlo radiation transport code developed by the Los Alamos National Laboratory (NM, USA). MCNPX is designed to simulate the behavior of particles, such as neutrons, photons, and electrons, as they interact with matter. It uses Monte Carlo methods to simulate the trajectories of individual particles through the material, considering various physical processes, such as scattering and absorption. MCNPX can model complex geometries and materials and can be used to calculate radiation dose rates, neutron fluxes, and other radiation transport-related quantities [51]. MCNPX is widely used in nuclear engineering, radiation protection, medical physics, and other fields that involve radiation transport. It has been validated against experimental data and is a highly reliable tool for simulating the transport of particles through matter. The present investigation involves the modeling of five distinct samples of lithium silicate glass in the form of discs, based on their respective elemental composition and density. The F4 Tally Meshes were positioned both frontally and backward to the absorber glass that was modeled [51], thereby yielding the mean gamma flux measurement. Figure 1a depicts a two-dimensional representation of the modeled structure, while Figure 1b displays a tri-dimensional view of the two-dimensional configuration. The ratios of primary and secondary gamma-ray flux values were

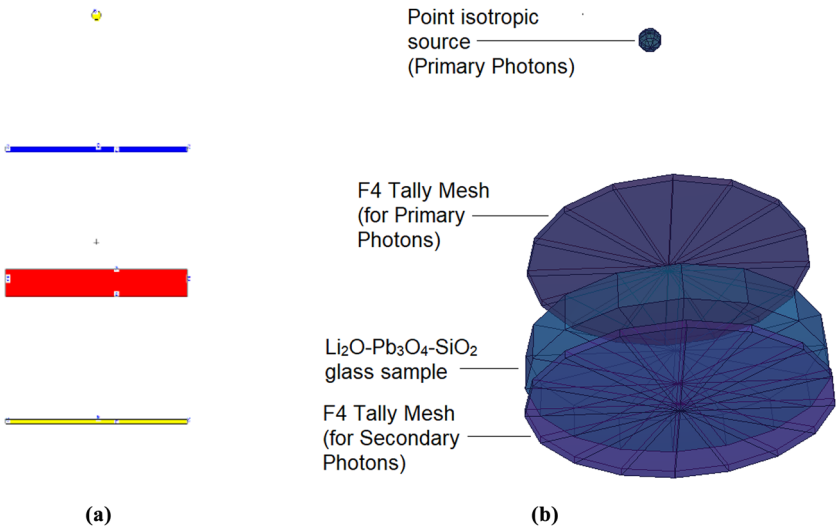

Figure 1: (a) 2-D view of the designed MCNPX simulation setup. (b) 3-D illustration of the designed MCNPX setup (2-D and 3-D views are obtained from MCNPX Visual Editor VisedX22S).

determined using the setup, and subsequently, the TF values were computed as outlined in the previous section. The study did not utilize the bit cut-off technique. The mode for tracking radiation has been configured to exclusively detect photons, while the tracking of neutrons and electrons has been deactivated. The simulation's efficiency was attempted to be enhanced, and the error rate was kept minimal by inhibiting the tracking of particles that do not impact the calculations. Furthermore, LENOVO P620 has been utilized for simulating operations in a workstation of general purpose.

3 Results and discussions

A key consideration in electromagnetic radiation shielding against types like gamma rays and X-rays is the density of the materials that are used. This is because the incident radiation interacts more closely with the surrounding electrons due to the large mass, increasing the likelihood that it will be absorbed. Figure 2 displays the densities of the five distinct lithium silicate glasses that were tested in this study. The figure illustrates how, depending on the glass composition, the density of the S1–S5 samples changed visibly. The S5 glass with a 0.4 mol% Ag_2O addition has the greatest density of these five lithium silicate glasses (Table 1). Linear attenuation coefficients (μ) refer to a shielding parameter depending on density. The linear attenuation coefficients (μ) of the examined lithium silicate glasses are shown in Figure 3a as a function of energy. All glass samples obtained their highest μ values in the low energy range, as seen in the figure. This is due to a quantitative excess of absorption per unit distance exposed to low-energy photons interacting with the glass. The Compton scattering phenomenon stands out as the predominant kind of interaction, which varies as energy levels increase. Gamma- or X-ray photons may spend part of their energy in this area on the ionization process in addition to going through a series of interactions before having all their energy absorbed. The fact that less energy is emitted per unit of distance in this region compared to the low-energy field, along with an increase in the penetrating qualities of energetic photons, maybe the cause of the lower m values in this region. The lithium silicate glass with 0.4 mol% Ag_2O doped, however, had the highest μ value among the examined lithium silicate glasses. The same applies to the values of mass attenuation coefficients (μ_m),

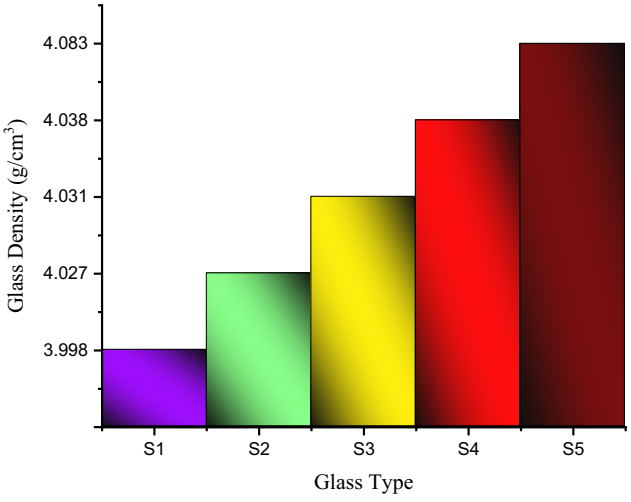

Figure 2: Variation of glass densities under investigation.

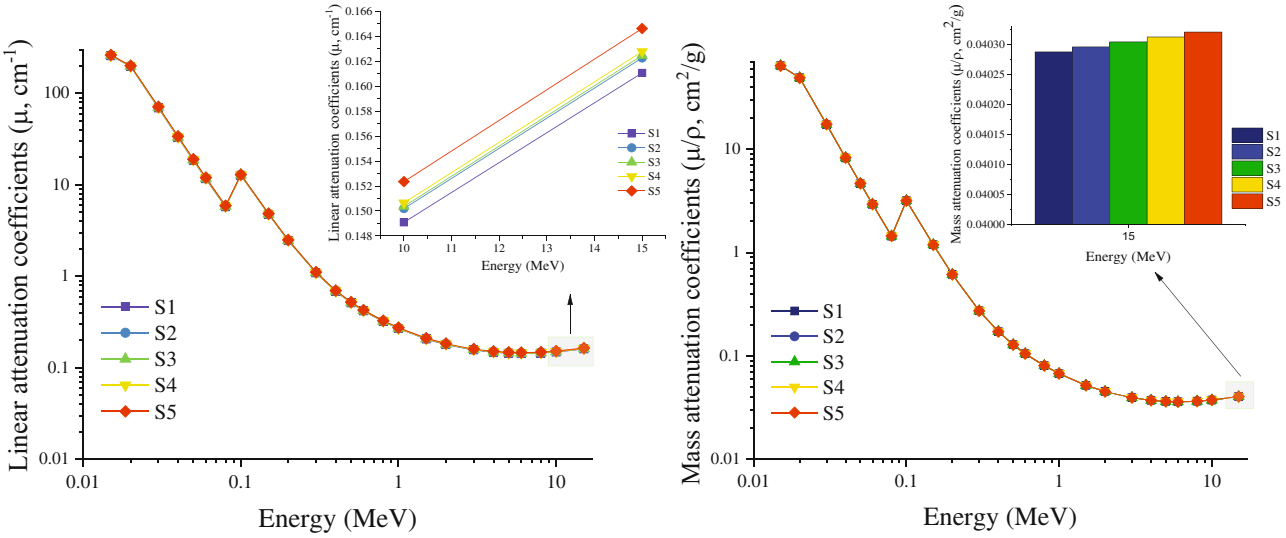

Figure 3: Variations of (a) linear and (b) mass attenuation coefficients with photon energy (MeV) for all S1–S5 glasses.

a parameter independent of density. The energy-dependent variations of the μ_m values for the S1–S5 glasses are shown in Figure 3b. The sample that removed the most gamma rays in this case, quantitatively and in terms of its atomic structure, was the 0.4 mol% Ag_2O-doped S5 sample. The variations in the HVL values for S1 to S5 samples according to the energy change are shown in Figure 4a. HVL values, which exhibited a negligible trend in the area of low energy, tended to increase concurrently with an increase in energy. This is because low-energy photons' limited penetrating properties allow them to be slit quantitatively at extremely thin layers. However, the increasing thickness value required to halve the corresponding gamma rays increase along with the increased penetrating capacity with the increase in energy. This also applies to the tenth value layer (TVL) values in Figure 4b. Among the eyeglasses inspected, sample S5 had the lowest HVL and TVL values. This has a constant association with the HVL value's linear attenuation coefficient values. Since HVL and TVL values are a reversal function of the linear attenuation coefficient, minimal HVL and TVL values were obtained for S1 with maximum linear attenuation coefficient values. These findings indicate that the S5 sample will, at the minimal material thickness values, give a quantitative halving of the gamma rays changing in the 0.015–15 MeV energy range. The important finding relates to the S5 sample's more significant protective capabilities.

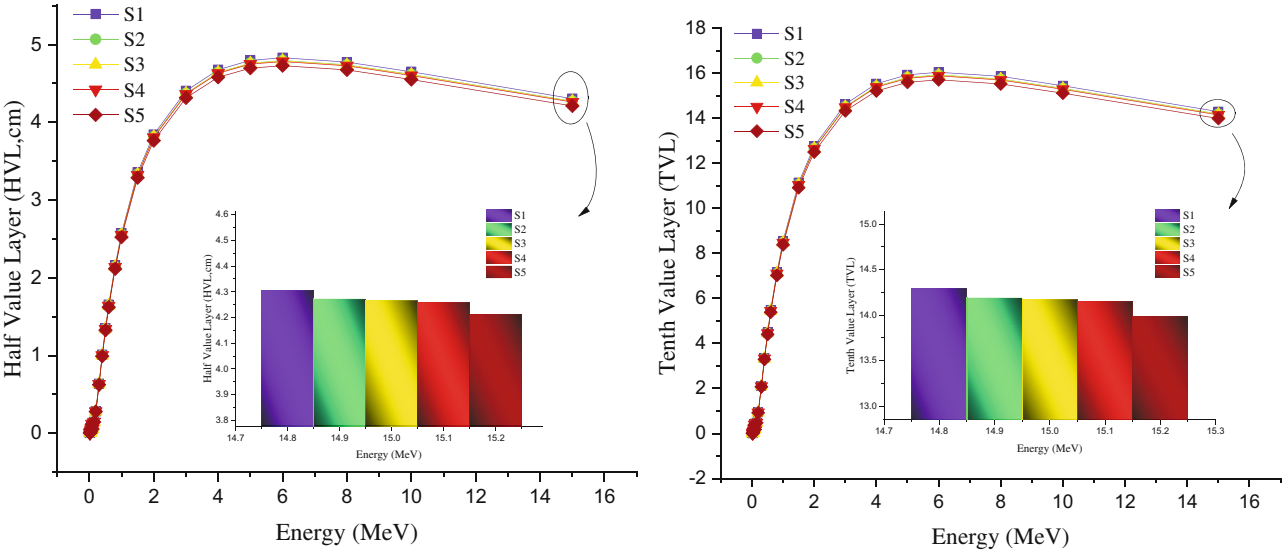

Figure 4: Variations of (a) half and (b) TVL (cm) with photon energy (MeV) for all S1–S5 glasses.

The term "mean free path" (MFP) refers to the typical distance that must be traveled by a gamma ray within a given material in order to undergo two consecutive interactions. The diminution of this parameter toward its minimum level denotes a smaller gap between the two interactions, leading to an increased efficacy of the absorption process. The MFP values obtained for the S1–S5 glasses exhibit energy-dependent variation trends, as illustrated in Figure 5. The MFP curve exhibits analogous traits to the HVL and TVL data in principle. The S5 sample exhibits minimal MFP values. This suggests that the mean displacement of a single gamma ray during two successive interactions will fall within the sample S5. The build-up factor is a crucial metric that can be established for materials utilized in radiation protection. The build-up factor may be defined with respect to individual energy levels and diverse MFP values. The value represents a metric that quantifies the frequency of collisions between photons during the interaction process occurring within the material. The extent to which a material absorbs photons is closely linked to the magnitude of the number of interactions the photons undergo. An elevated collision rate within a material can enhance the absorption process of energetic photons, thereby increasing their efficacy. On the other hand, if there is an absence or insufficiency of collisions within the material, the photons with high energy will be unable to transfer their energy, leading to an ineffective absorption process. The build-up factor is a metric that expresses the proportion of photons that have undergone collision versus those that have not, within a given material. The comparison of EBF and energy absorption build-up factor (EABF) values for samples S1–S5 at various

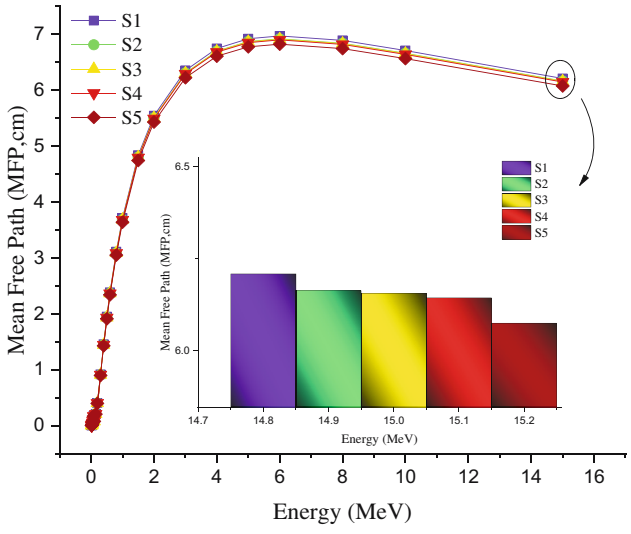

Figure 5: Variations of MFP (cm) with photon energy (MeV) for all S1–S5 glasses.

MFP values is illustrated in Figures 6 and 7. The figure demonstrates that the energy value exerts a notable impact on the alteration of EBF and EABF values across all specimens. This phenomenon can be attributed to the prevailing mode of interaction resulting from the photon energy as expounded upon in the preceding sections. The sample denoted as S5 exhibited the lowest values for both EBF and EABF among the samples that were analyzed. This phenomenon can be elucidated by the observation that the quantity of photons that have undergone collision in S5 is comparatively greater than that in the remaining samples. The surplus quantity of photons that have undergone collision may be regarded as a beneficial factor in the process of absorption. The final parameter analyzed in this investigation was the TF values. The aforementioned values were acquired utilizing the MCNPX code and were determined through proportional assessments of the photon quantity that enters and traverses the sample. The TF values for samples S1–S5 at varying sample thicknesses and radioisotope energies are depicted in Figure 8a–c. The figure illustrates that the TF amounts reach their maximum values for each radioisotope energy when the material thickness is low. A negative correlation is observed between the increase in thickness and the aforementioned values. This pertains to the phenomenon of diminishing secondary photon quantity as the thickness of the material increases. To clarify, it is anticipated that the TF values will decrease due to increased absorption in thicker materials. The S5 sample exhibits minimal TF values at every radioisotope energy and material thickness. The aforementioned parameters, which were derived through theoretical means and expounded upon in preceding sections, are congruent with an autonomous Monte Carlo simulation phase. The study found that sample S5 yielded the most efficient results for all parameters analyzed. Hence, the suggested configuration for S5 can be deemed as the most efficacious configuration for a lithium silicate glass framework concerning its capacity to absorb gamma rays.

4 Conclusion

It is commonly known that Pb and Pb-based shields have the best photon shielding qualities. However, recent studies revealed that Pb-based materials have several serious limitations, including toxicity, poor durability, opaqueness, and high cost. The search for alternate radiation shielding materials has accelerated in recent years. This research sought to investigate more environmentally friendly radiation shielding materials for nuclear medical facilities

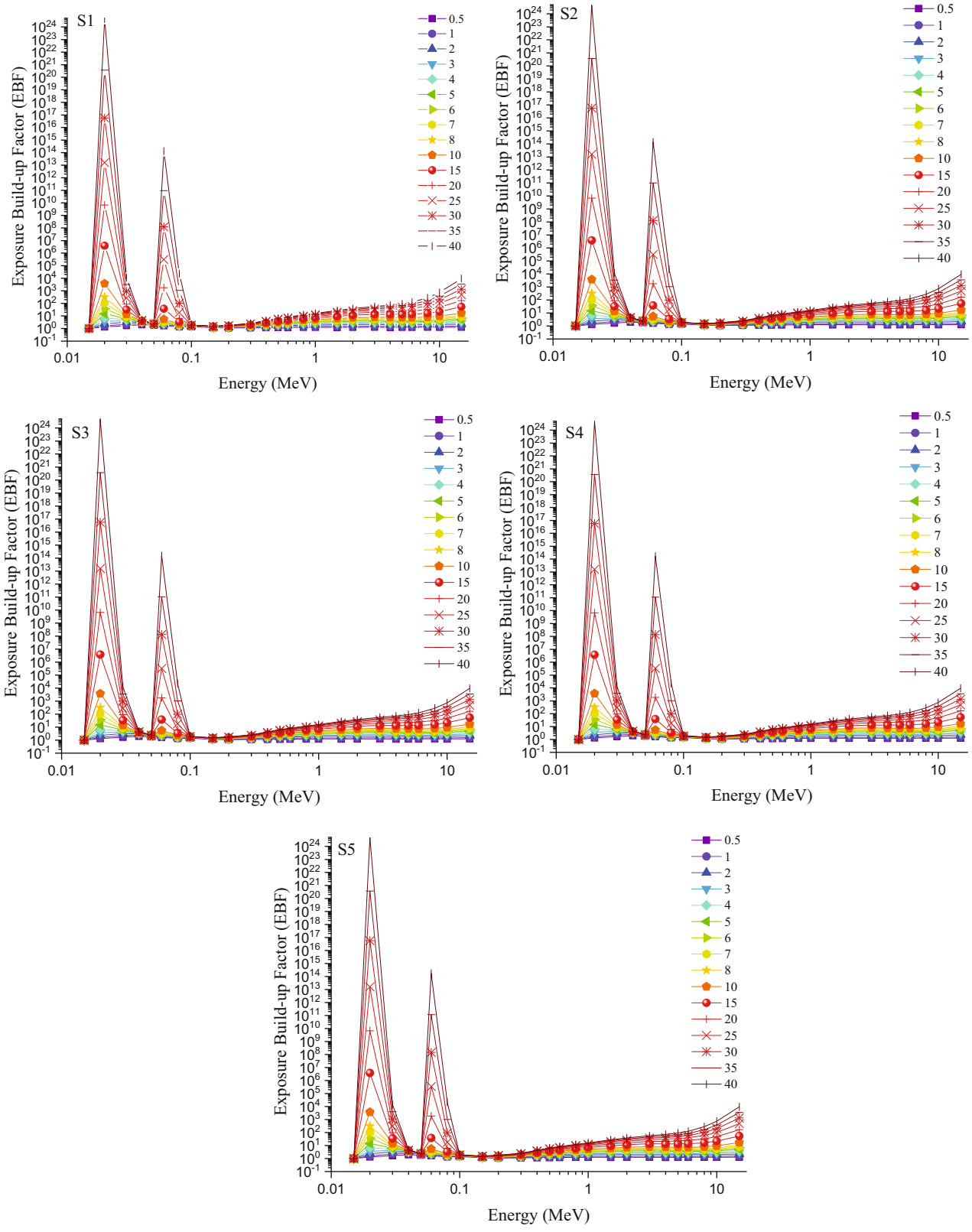

Figure 6: Variation of EBFs of investigated glasses at different MFP values.

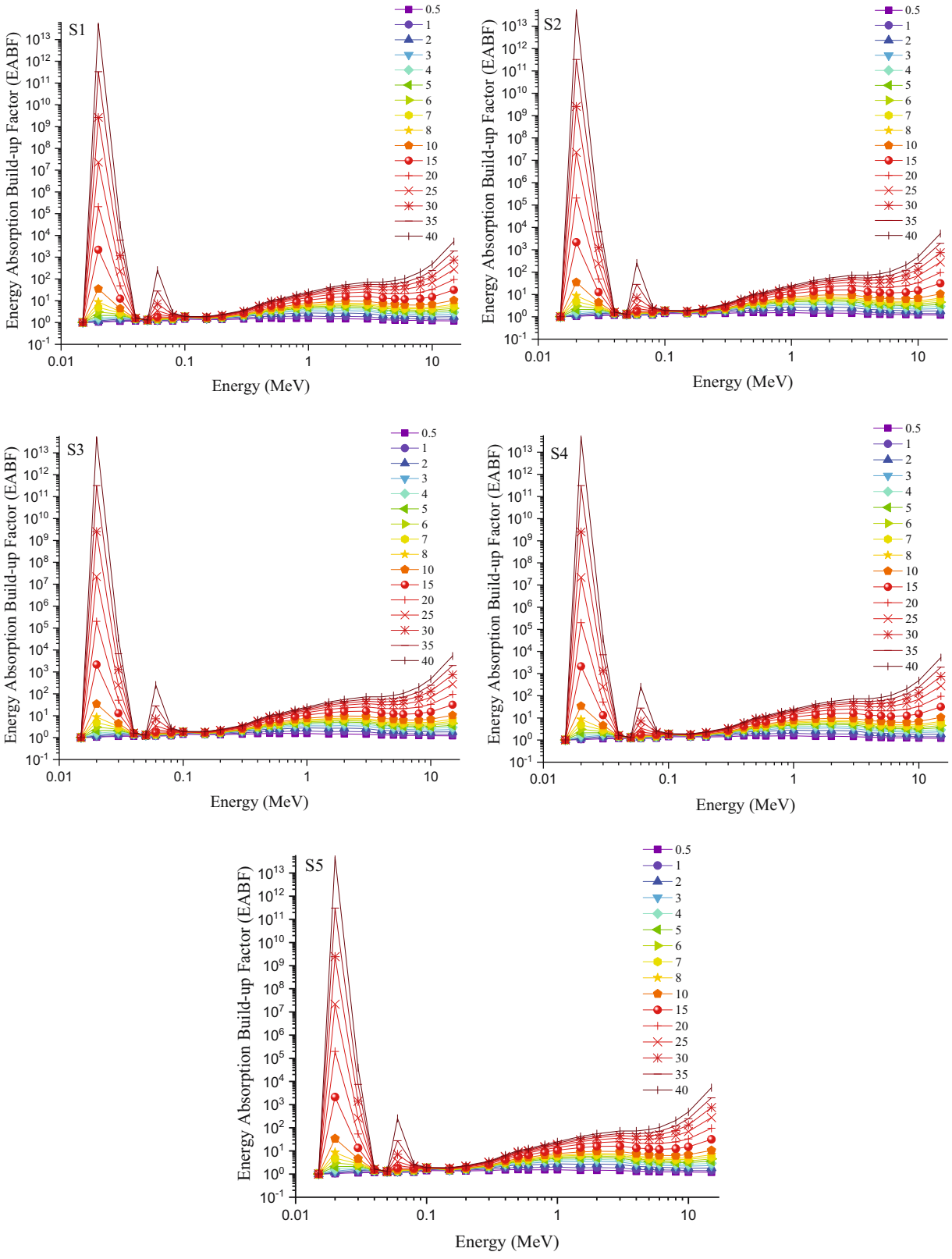

Figure 7: Variation of EABFs of investigated glasses at different MFP values.

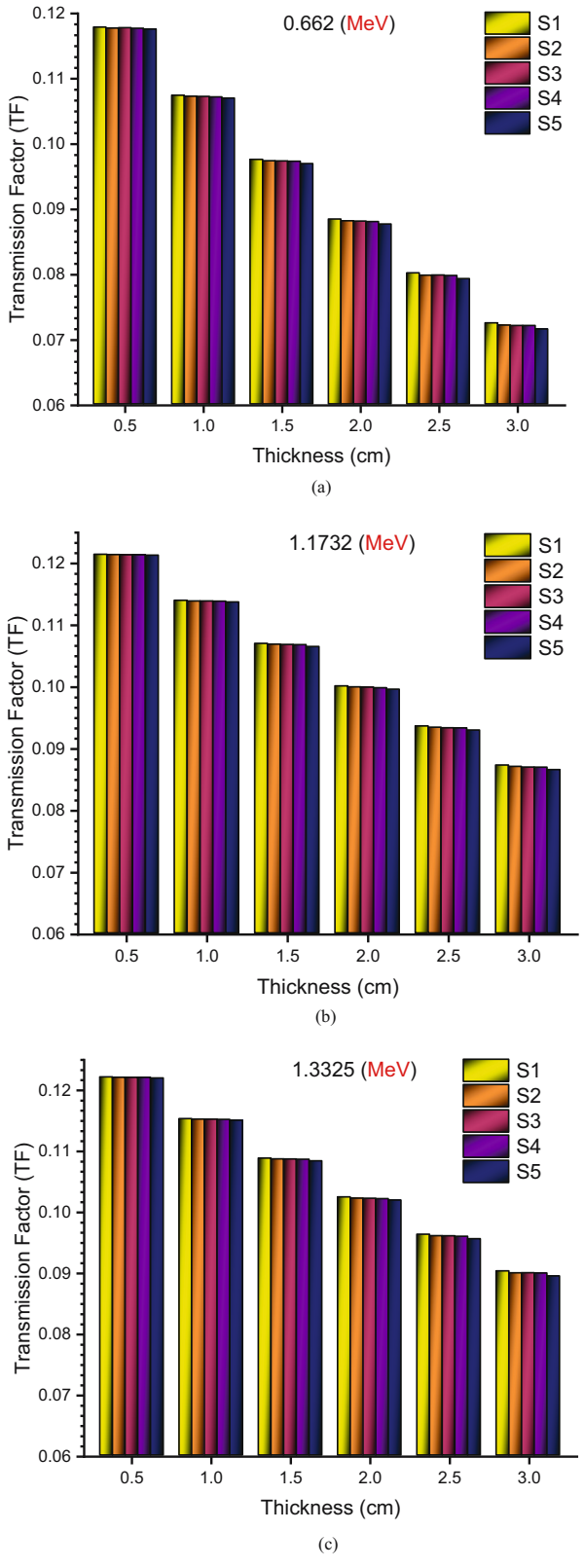

Figure 8: TFs of investigated glasses as a function of used radioisotope energies: (a) 0.662 MeV, (b) 1.1732 MeV, and (c) 1.3325 MeV at different glass thicknesses.

considering recent studies on radiation protection. The quantitative results that would be obtained as a result of such a study could offer important details regarding how the tested material behaves when in use. The examination of the glass composition of Li_2O–Pb_3O_4–SiO_2 has been the main topic of this article with various compositions to explore the gamma-ray attenuation characteristics of S1–S5 samples. It is well known that adding Ag_2O makes glass structures more stable and drastically alters their physical characteristics, such as density and molar volume. We have concentrated on the radiation shielding properties of five samples from the glass series because adding more Ag_2O to a glass structure with a Li_2O–Pb_3O_4–SiO_2 composition would increase the glass density as well as change and improve the radiation shielding properties of the incorporated glass sample. We compared the gamma-ray attenuation shielding properties of five glasses from the glass system over a wide range of input photon energy. Variations of the linear (μ) and mass attenuation coefficients (μ/ρ), HVL, TVL, and MFP of the examined glass samples have been determined using the general-purpose Monte Carlo code MCNPX. With the help of the Phy-X/PSD program, the computed results for mass attenuation coefficients were compared for energies between 0.015 and 15 MeV. Using the G–P fitting method at various MFP values, the EBF and EABF values of the examined glasses were calculated. Furthermore, the TFs of the examined glasses in relation to the radioisotope energies of 0.662, 1.1732, and 1.3325 MeV at various glass thicknesses have been determined. Low values for the shielding parameters HVL, TVL, MFP, EBF, and EABF, as well as high values for the MAC, indicate that the glass material has effective shielding qualities. The lowest value for the HVL and the highest values of the MAC for the gamma reaction both occurred at low energy of 15 keV. On the other hand, the lowest values of the above-mentioned parameters occurred at an energy of 15 MeV. Our results indicate that the S5 sample, which has the greatest mol% Ag_2O content and has the highest linear (μ) and mass (μ/ρ) attenuation coefficients across the board, is an ideal option for gamma protection. In conclusion, additional research on the effects of Ag_2O additive for nuclear radiation shielding applications in various glass systems is possible. We offered comprehensive findings in this study after considering a number of variables. The suggested glassy system has potential but due to the extensive material characteristics of glass materials, it will require ongoing optimization and refinement. Based on the information presented, a broad overview of the glass samples with Ag_2O incorporation was given. The major material features connected to glass components, however, necessitate continued study in terms of overall optimization and development for the suggested glass system.

Acknowledgement: The authors would like to express their deepest gratitude to Princess Nourah bint Abdulrahman University Researchers Supporting Project number (PNURSP2023R149), Princess Nourah bint Abdulrahman University, Riyadh, Saudi Arabia.

Funding information: This research was funded by Princess Nourah bint Abdulrahman University Researchers Supporting Project number (PNURSP2023R149), Princess Nourah bint Abdulrahman University, Riyadh, Saudi Arabia.

Author contributions: H.O.T. – conceptualization, writing – original draft, supervision, writing – review and editing; G.A. – visualization, software, writing– original draft; H.M.H.Z. – formal analysis, data curation; E.R. – data curation, formal analysis, writing – original draft; G.K. – data curation, formal analysis, writing – original draft; E.I. – data curation, formal analysis, writing – original draft; D.S.B. – visualization, software; and G.S.D. – visualization, software, writing – original draft; A.E – methodology, funding acquisition (A.E. would like to thank "Dunarea de Jos" University of Galati, Romania, for the material and technical support).

Conflict of interest: Authors state no conflict of interest.

Ethical approval: The conducted research is not related to either human or animal use.

Data availability statement: The datasets generated during and/or analyzed during the current study are available from the corresponding author on reasonable request.

References

[1] Abo-Mosallam HA, Ibrahim S, Mahdy EA. New high nickel-containing glass-ceramics based on Li_2O–CaO–SiO_2 eutectic (954°C) system for magnetic applications. J Non-Cryst Solids. 2022;80:121385. doi: 10.1016/j.jnoncrysol.2021.121385.

[2] Elliott SR. Physics of amorphous materials. London: Longman; 1990.

[3] Zhang P, Li X, Yang J, Xu S. Effect of heat treatment on the microstructure and properties of lithium disilicate glass-ceramics. J Non-Cryst Solids. 2014;402:101–5. doi: 10.1016/j.jnoncrysol.2014.05.023.

[4] Shelby JE. Introduction to glass science and technology. Royal Society. Cambridge: RSC Press; 1997.

[5] Holand W, Beall G. Glass-ceramic technology. Westerville, OH: American Ceramic Society; 2002.

[6] Elbatal FH, Azooz MA, Hamdy YM. Preparation and characterization of some multicomponent silicate glasses and their glass–ceramics derivatives for dental applications. Ceram Int. 2009;35:1211. doi: 10.1016/j.ceramint.2008.06.009.

[7] Elbatal HA, Mandouh Z, Zayed H, Marzouk SY, Elkomy G, Hosny A. Gamma ray interactions with undoped and CuO-doped lithium disilicate glasses. Phys B: Condens Matter. 2010 Dec 1;405(23):4755–62. doi: 10.1016/j.physb.2010.08.071.

[8] Lawita P, Thepsuwan W. Characterization and properties of lithium disilicate glass ceramics in the SiO_2-Li_2O-K_2O-Al_2O_3 system for dental applications. Adv Mater Sci Eng. 2013;763838, 11 pages. Hindawi Publishing Corporation. doi: 10.1155/2013/763838.

[9] Baumgartner S, Gmeiner R, Schönherr JA, Stampfl J. Stereolithography-based additive manufacturing of lithium disilicate glass ceramic for dental applications. Mater Sci Eng C. 2020 Nov;116:111180. doi: 10.1016/j.msec.2020.111180.

[10] Krüger S, Deubener J, Ritzberger C, Höland W. Nucleation kinetics of lithium metasilicate in ZrO_2-bearing lithium disilicate glasses for dental application. Int J Appl Glass Sci. 2013;4(1):9–19. doi: 10.1111/ijag.12011.

[11] Meng M, Wang XS, Li KY, Deng ZX, Zhang ZZ, Sun YL, et al. Effects of surface roughness on the time-dependent wear performance of lithium disilicate glass ceramic for dental applications. J Mech Behav Biomed Mater. 2021 Sep;121:104638. doi: 10.1016/j.jmbbm.2021.104638.

[12] Charles RJ. Some structural and electrical properties of lithium silicate glasses. J Am Ceram Soc. 1963 May;46(5):235–8. doi: 10.1111/j.1151-2916.1963.tb19779.x.

[13] Gomaa M, Darwish H, Salman SM. Electrical properties of some Y_2O_3 and/or Fe_2O_3 -containing lithium silicate glasses and glass-ceramics. J Mater Sci Mater Electron 19(1):5–15. doi: 10.1007/s10854-007-9288-3.

[14] Biskri ZE, Rached H, Bouchear M, Rached D. Computational study of structural, elastic and electronic properties of lithium disilicate ($Li_2Si_2O_5$) glass-ceramic. J Mech Behav Biomed Mater. 2014 April;32:345–50. doi: 10.1016/j.jmbbm.2013.10.029.

[15] Arya SK, Danewalia SS, Singh K. Frequency independent low-k lithium borate nanocrystalline glass ceramic and glasses for microelectronic applications. J Mater Chem C. 2016;4:3328–36. doi: 10.1039/C5TC03364K.

[16] Singh VP, Badiger NM, Kaewkhao J. Radiation shielding competence of silicate and borate heavy metal oxide glasses: comparative study. J Non-Cryst Solids. 2014;404:167–73. doi: 10.1016/j.jnoncrysol.2014.08.003.

[17] Marzouk MA, Elbatal FH, Eisa WH, Ghoneim NA. Comparative spectral and shielding studies of binary borate glasses with the heavy metal oxides SrO, CdO, BaO, PbO or Bi_2O_3 before and after gamma irradiation. J Non-Cryst Solids. 2014;387:155–60. doi: 10.1016/j.jnoncrysol.2014.01.002.

[18] Abousehly A, Issa SAM, El-Oyoun MA, Afify N. Electrical and mechanical properties of Li_2O–BaO–B_2O_3 glass system. J Non-Cryst Solids. 2015;429:148–52. doi: 10.1016/j.jnoncrysol.2015.09.003.

[19] Issa SAM, Sayyed MI, Zaid MHM, Matori KA. Photon parameters for gamma-rays sensing properties of some oxide of lanthanides. Results Phys. 2018;9:206–10. doi: 10.1016/j.rinp.2018.02.039.

[20] Issa SAM, Darwish AAA, El-Nahass MM. The evolution of gamma-rays sensing properties of pure and doped phthalocyanine. Prog Nucl Energy. 2017;100:276–82. doi: 10.1016/j.pnucene.2017.06.016.

[21] Kurtuluş R, Kavas T, Gayret A, Biçeroğlu D. Physical, optical and radiation-shielding features of CeO2-reinforced Li_2O–ZnO–SiO_2 glass. Emerg Mater Res 2022;11(1):86–92. doi: 10.1680/jemmr.21.00022.

[22] Malidarre RB, Tekin HO, Gunoglu K, Akyildirim H. Assessment of gamma ray shielding properties for skin. Int J Comput Exp Sci Eng. 2023;9(1):6–10. doi: 10.22399/ijcesen.1247867.

[23] ALMisned G, Baykal DS, Ilik E, Abuzaid M, Kilic G, Tekin HO. Functional assessment of various rare-earth (RE) ion types: An investigation on gamma-ray attenuation properties of GeO_2-$B2O_3$-$P2O_5$-ZnO-Tb_2O_3-RE magneto-optical glasses. Optik. 2023 March;274:170526. doi: 10.1016/j.ijleo.2023.170526.
[24] Rashad M, Tekin HO, Zakaly HM, Pyshkina M, Issa SAM, Susoy G. Physical and nuclear shielding properties of newly synthesized magnesium oxide and zinc oxide nanoparticles. Nucl Eng Technol. 2020;52(9):2078–84. doi: 10.1016/j.net.2020.02.013.
[25] Issa SAM, Ali AM, Tekin HO, Saddeek YB, Al-Hajry A, Algarni H, et al. Enhancement of nuclear radiation shielding and mechanical properties of $YBiBO_3$ glasses using La_2O_3. Nucl Eng Technol. 2020;52(6):1297–303. doi: 10.1016/j.net.2019.11.017.
[26] ALMisned G, Baykal DS, Susoy G, Kilic G, Zakaly HMH, Ene A, et al. Determination of gamma-ray transmission factors of WO_3–TeO_2–B_2O_3 glasses using MCNPX Monte Carlo code for shielding and protection purposes. Appl Rheol. 32(1):166–77. doi: 10.1515/arh-2022-0132.
[27] ALMisned G, Baykal DS, Kilic G, Susoy G, Zakaly HMH, Ene A, et al. Assessment of the usability conditions of Sb_2O_3–PbO–B_2O_3 glasses for shielding purposes in some medical radioisotope and a wide gamma-ray energy spectrum. Appl Rheol. 32(1):178–89. doi: 10.1515/arh-2022-0133.
[28] Almisned G, Akkurt I, Tekin HO, Yuksek I, Ekmekçi I. Variation in gamma ray shielding properties of glasses with increasing boron oxide content. Radiochim Acta 111(3):217–23.
[29] ALMisned G, Rabaa E, Baykal DS, Ilik E, Kilic G, Zakaly HMH, et al. The impact of chemical modifications on gamma-ray attenuation properties of some WO3-reinforced tellurite glasses. Open Chem. 2023;21(1):20220297. doi: 10.1515/chem-2022-0297.
[30] Tekin HO, Susoy G, Issa SAM, Ene A, ALMisned G, Rammah YS, et al. Heavy Metal Oxide (HMO) glasses as an effective member of glass shield family: A comprehensive characterization on gamma ray shielding properties of various structures. J Mater Res Technol. 2022 May–June;18:231–44. doi: 10.1016/j.jmrt.2022.02.074.
[31] Ortiz López P, Dauer LT, Loose R, Martin CJ, Miller DL, Vañó E, et al. Authors on Behalf of ICRP, Occupational radiological protection in interventional procedures. ICRP Publication 139. Ann ICRP. 2018;47(2):1–118. doi: 10.1177/0146645317750356.
[32] Singer G. Occupational radiation exposure to the surgeon. J Am Acad Orthop Surg. 2005;13(1):69–76. doi: 10.5435/00124635-200501000-00009.
[33] Lambert K, McKeon T. Inspection of lead aprons: Criteria for rejection. Health Phys. 2001 May;80(5 Suppl):S67–9. doi: 10.1097/00004032-200105001-00008.
[34] Giordano BD, Baumhauer JF, Morgan TL, Rechtine GR, II. Patient and surgeon radiation exposure: Comparison of standard and mini-Carm fluoroscopy. J Bone Jt Surg Am. 2009;91(2):297–304. doi: 10.2106/JBJS.H.00407.
[35] Radiation Safety in Well Logging, International Atomic Energy Agency; Vienna; 2020. (IAEA safety standards series, No. SSG-57, Specific Safety Guides).
[36] Lambert K, McKeon T. Inspection of lead aprons: Criteria for rejection. Operational radiation safety. Health Phys. 2001 May;80(supplement 5):S67–9. doi: 10.1097/00004032-200105001-00008.
[37] Protection and security of radiation sources, page last reviewed/updated Friday; March 27, 2020, https://www.nrc.gov/about-nrc.html.
[38] Keerti Kut TVN, Marijan S, Pisk J, Venkata Sekhar A, Siva Sesha Reddy A, Venkatramaiah N, et al. Impact of silver ions on dielectric properties and conductivity of lithium silicate glass system mixed with red lead. J Non-Cryst Solids. 2022;588:121641. doi: 10.1016/j.jnoncrysol.2022.121641.
[39] Şakar E, Özpolat Ö, Alım B, Sayyed M, Kurudirek M. Phy-X/PSD: development of a user friendly online software for calculation of parameters relevant to radiation shielding and dosimetry. Radiat Phys Chem. 2020;166:108496. doi: 10.1016/j.radphyschem.2019.108496.
[40] Gowda S, Krishnaveni S, Yashoda T, Umesh TK, Gowda R. Photon mass attenuation coefficients, effective atomic numbers and electron densities of some thermoluminescent dosimetric compounds. Pramana. 2004;63:529–41. doi: 10.1007/BF02704481.
[41] Elmahroug Y, Tellili B, Souga C. Determination of total mass attenuation coefficients, effective atomic numbers and electron densities for different shielding materials. Ann Nucl Energy. 2015;75:268–74. doi: 10.1016/j.anucene.2014.08.015.
[42] Kavaz E, Tekin HO, Agar O, Altunsoy EE, Kilicoglu O, Kamislioglu M, et al. The Mass stopping power/projected range and nuclear shielding behaviors of barium bismuth borate glasses and influence of cerium oxide. Ceram Int. 2019;45:15348–57. doi: 10.1016/j.ceramint.2019.05.028.
[43] Ekinci N, Kavaz E, Özdemir Y. A study of the energy absorption and exposure buildup factors of some anti-inflammatory drugs. Appl Radiat Isot. 2014;90:265–73. doi: 10.1016/j.apradiso.2014.05.003.
[44] Singh VP, Badiger NM, Chanthima N, Kaewkhao J. Evaluation of gamma-ray exposure buildup factors and neutron shielding for bismuth borosilicate glasses. Radiat Phys Chem. 2014;98:14–21. doi: 10.1016/j.radphyschem.2013.12.029.
[45] Oto B, Gulebaglan SE, Madak Z, Kavaz E. Effective atomic numbers, electron densities and gamma rays buildup factors of inorganic metal halide cubic perovskites $CsBX_3$ (B = Sn, Ge; X = I, Br, Cl). Radiat Phys Chem. 2019;159:195–206. doi: 10.1016/j.radphyschem.2019.03.010.
[46] Tekin HO, ALMisned G, Susoy G, Zakaly HMH, Issa SAM, Kilic G, et al. A detailed investigation on highly dense CuZr bulk metallic glasses for shielding purposes. Open Chem. 2022;20(1):69–80. doi: 10.1515/chem-2022-0127.
[47] Tekin HO, ALMisned G, Zakaly HMH, Zamil A, Khoucheich D, Bilal G, et al. Gamma, neutron, and heavy charged ion shielding properties of Er_3+ -doped and Sm_3+ -doped zinc borate glasses. Open Chem. 2022;20(1):130–45. doi: 10.1515/chem-2022-0128.
[48] Choudhary MD, Akkurt I, Almisned G, Tekin HO. Radiation-shielding properties of titanium dioxide-added composites. Emerg Mater Res. 2022 September;11(3):319–24. doi: 10.1680/jemmr.22.00054.
[49] Sayyed MI, Tekin HO, Malaa M, Taki MHA, Mhareb O, Agar E, et al. Bi2O3-B2O3-ZnO-BaO-Li_2O glass system for gamma ray shielding applications. Optik. 2020;201:163525. doi: 10.1016/j.ijleo.2019.163525.
[50] Kaewjaeng S, Kothan S, Chanthima N, Kim HJ, Kaewkhao J. Gamma radiation shielding materials of lanthanum calcium silicoborate glasses. Mater Today Proc. 2018;5(7):14901–6. doi: 10.1016/j.matpr.2018.04.027.
[51] RSICC computer code collection, MCNPX'User's manual Version 2.4.0. Monte Carlo N-particle transport code system for multiple and high energy applications; 2002.